Solve Kinetic Equations with Deep Learning

Zheng Ma

Shanghai Jiao Tong University

Joint work with Shi Jin, Keke Wu, Tianai Zhang, Han Wang, Jingrun Chen

July 20, 2025

Introduction

Kinetic equations are important in many areas

Neutron transport

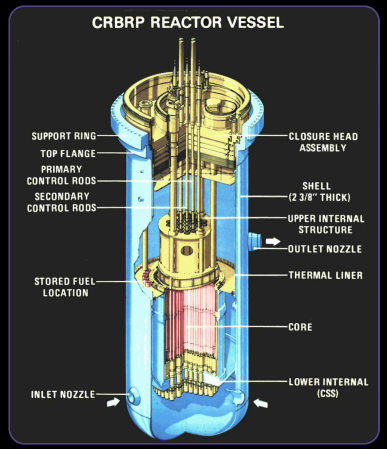

Fission reactor

Radiative transfer

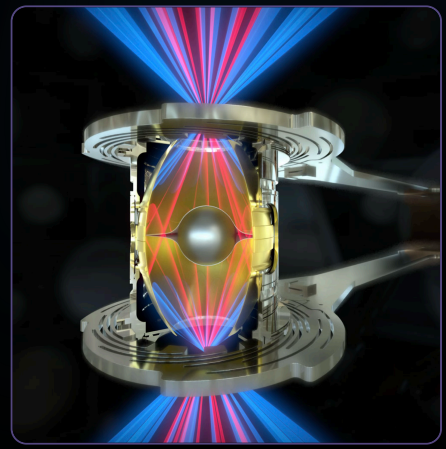

ICF

Rarefied gas

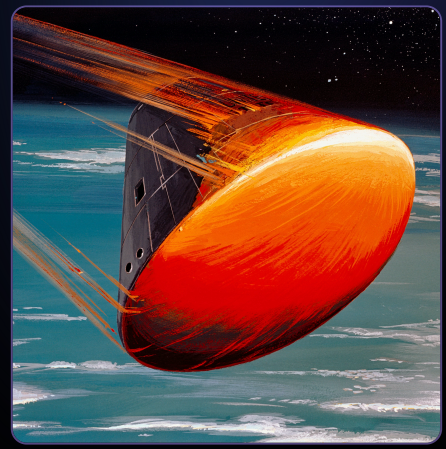

Reentry

Key problem: numerical simulation of kinetic equations

Multiscale Kinetic Equations

$$\partial_t f + v \cdot \nabla_x f = Q(f)$$

- $f(t, x, v)$: distribution function at time t in phase sapce (x, v)
- $Q(f)$: collision operator
- ε: Knudsen number (ratio between mean free path and characteristic length)

Neutron transport equation

$$\varepsilon \partial_t f + v \cdot \nabla_x f + \Sigma_t f = \frac{1}{\varepsilon} \int \Sigma_s(v, v') f \, \mathrm{d}v' + q$$

BGK equation

$$\partial_t f + v \cdot \nabla_x f = \frac{1}{\varepsilon} \left(M_{\mathrm{eq}}[f] - f \right)$$

Multiscale problem: ε can vary from $O(1)$ kinetic regime to 0 hydrodynamic regime

Numerical Chanllenges

Curse of dimensionality

Dimension

- Phase space + time: 6 + 1 = 7
- Collision operator is a 5-fold integral
- Need to evalute collision at every phase point

Collision

- Hard to maintain conservation at discrete level
- Highly nonlinear for Boltzmann collision
- Ray effect

Multiscale

- Stability issues for small ε (stiffness)
- Consistency of the scheme with limiting model as $\varepsilon \to 0$
- Automatically capture the transition across regimes

Conventional Approaches

Probabilistic approaches

- Monte Carlo methods for linear transport
  - MCNP
  - COG (LLNL, criticality safety analysis, general radiation)
  - Mercury
- Direct simulation Monte Carlo (DSMC) methods
  - Bird, Nanbu, ...
  - Sparta (ORNL, rarefied gas dynamics)

Pros

- Easy implementation
- Relatively efficient

Cons

- Only half-order accuracy
- Converge slow
- Random fluctuations

Conventional Approaches

Deterministic approaches

- Discrete velocity/ordinate methods (DVM)
  - Ardra (LLNL)
  - NEWT (ORNL)
  - DORT
  - Kit-RT
- Spectral methods

Pros

- Spectral accuracy
- Relatively expensive

Cons

- Do not maintain conservation

Deep learning methods may become new approach

Overcome the curse of dimensionality

Solve PDEs with Deep Learning

Key components

Constraints as the loss of minimization problem

- Model: PDE / physical information needed (e.g., PINNs, DeepRitz, DeepGalerkin)
- Data: pure supervised or as a priori information
- IC (initial conditions) and BC (boundary conditions)
- Other constraints: conservation, symmetry, etc.

Architecture build a deep neural network (function class) as the trial function

- Approximate solution: PINNs, DeepRitz, DeepGalerkin, etc.
- Approximate solution operator: DeepONet, FNO, etc.
- Mapping from equations (as a computational graph) to solutions (PDEFormer)

Optimization

- Minimize loss over the parameter space, usually SGD, Adam, LBFGS, etc.

Constraints for multiscale kinetic equations

PINNs, DeepRitz, etc.

Linear Transport Equation

1-D for illustration

$$\varepsilon \partial_t f + v \cdot \nabla_x f = \frac{1}{\varepsilon} \left(\frac{1}{2} \int_{-1}^{1} f \, \mathrm{d}v' - f \right)$$

PINN for example:

- **Architecture**: approximate the solution by a deep neural network

$$f_\theta^{\mathrm{NN}}(t, x, v) \approx f(t, x, v)$$

- **Model**: take the least square of the linear transport equation residual (strong form) as loss

$$\mathcal{R}_{\mathrm{PINN}}^{\varepsilon} = \int \left(\varepsilon^2 \partial_t f_\theta^{\mathrm{NN}} + \varepsilon v \cdot \nabla_x f_\theta^{\mathrm{NN}} - \left(\frac{1}{2} \int_{-1}^{1} f_\theta^{\mathrm{NN}} \mathrm{d}v' - f_\theta^{\mathrm{NN}} \right) \right)^2 \mathrm{d}v \mathrm{d}x \mathrm{d}t$$

Result of PINN

$$\varepsilon \partial_t f + v \cdot \nabla_x f = \frac{1}{\varepsilon} (\rho(t,x) - f), \quad \rho(t,x) = \frac{1}{2} \int_{-1}^{1} f \, \mathrm{d}v'$$

Kinetic regime: $\varepsilon = 1$

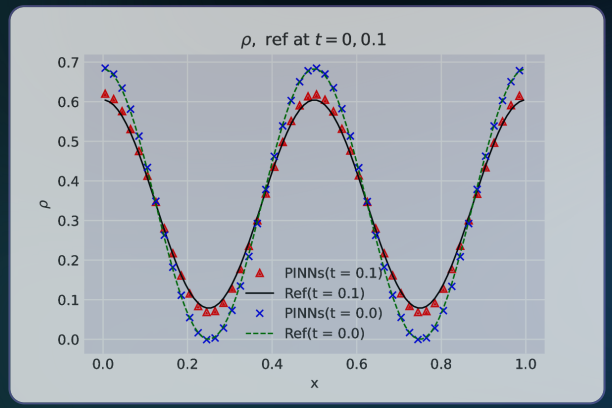

$$f_0(x,v) = [1 + \cos(4\pi x)] e^{-\frac{v^2}{2}} / \sqrt{2\pi}$$

Diffusive regime: $\varepsilon = 10^{-8}$

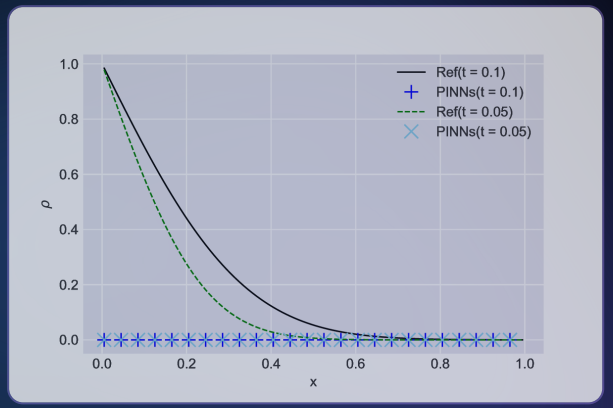

$$f_0(x,v) = 0$$

Failure of PINN Loss

PINN can not resolve small scale

$$\mathcal{R}^{\varepsilon}_{\mathrm{PINN}} = \int \left(\varepsilon^2 \partial_t f_\theta^{\mathrm{NN}} + \varepsilon v \cdot \nabla_x f_\theta^{\mathrm{NN}} - \left(\frac{1}{2} \int_{-1}^{1} f_\theta^{\mathrm{NN}} \mathrm{d}v' - f_\theta^{\mathrm{NN}} \right) \right)^2 \mathrm{d}v\mathrm{d}x\mathrm{d}t$$

Let $\varepsilon \to 0$

$$\mathcal{R}^{0}_{\mathrm{PINN}} = \int \left(\frac{1}{2} \int_{-1}^{1} f_\theta^{\mathrm{NN}} \mathrm{d}v' - f_\theta^{\mathrm{NN}} \right)^2 \mathrm{d}v\mathrm{d}x\mathrm{d}t$$

which can be viewed as the PINN loss of the steady equation

$$f_\theta^{\mathrm{NN}} = \frac{1}{2} \int_{-1}^{1} f_\theta^{\mathrm{NN}} \mathrm{d}v'$$

PINN loss is not AP (Asymptotic-preserving), i.e., it does not converge to the correct macroscopic limit as $\varepsilon \to 0$.

Diffusion Limit

$$\varepsilon \partial_t f + v \cdot \nabla_x f = \frac{1}{\varepsilon} (\rho(t,x) - f), \quad \rho(t,x) = \langle f \rangle := \frac{1}{2} \int_{-1}^{1} f \mathrm{d}v'.$$

Decompose f into the equilibrium $\rho(t,x)$ and the non-equilibrium part $g(t,x,v)$:

$$f(t,x,v) = \rho(t,x) + \varepsilon g(t,x,v),$$

where the non-equilibrium part g clearly satisfies $\langle g \rangle = 0$

Subsititing $f = \rho + \varepsilon g$ into the linear transport equation yields

$$\begin{cases} \partial_t \rho + \langle v \cdot \nabla_x g \rangle = 0, \\ \\ \varepsilon^2 \partial_t g + \varepsilon (I - \Pi)(v \cdot \nabla_x g) + v \cdot \nabla_x \rho = -g. \end{cases}$$

where I is the identity operator and $\Pi(\cdot)(v) := \langle \cdot \rangle$ is the projection operator.

Micro-macro System

Classical numerical schemes based on this system are usually AP schemes

The micro-macro system for the linear trasport equation

$$\begin{cases} \partial_t \rho + \langle v \cdot \nabla_x g \rangle = 0, \\ \\ \varepsilon^2 \partial_t g + \varepsilon \left(I - \Pi \right) \left(v \cdot \nabla_x g \right) + v \cdot \nabla_x \rho = -g. \end{cases}$$

Sending $\varepsilon \to 0$, the above system formally approaches

$$\begin{cases} \partial_t \rho + \langle v \cdot \nabla_x g \rangle = 0, \\ -v \cdot \nabla_x \rho = g. \end{cases}$$

Plugging the second equation into the first equation gives the diffusion equation

$$\rho_t - \frac{1}{3} \rho_{xx} = 0.$$

What is "good" loss for multiscale kinetic equations?

Conservation, symmetry, parity, etc.

Asymptotic-Preserving Neural Networks

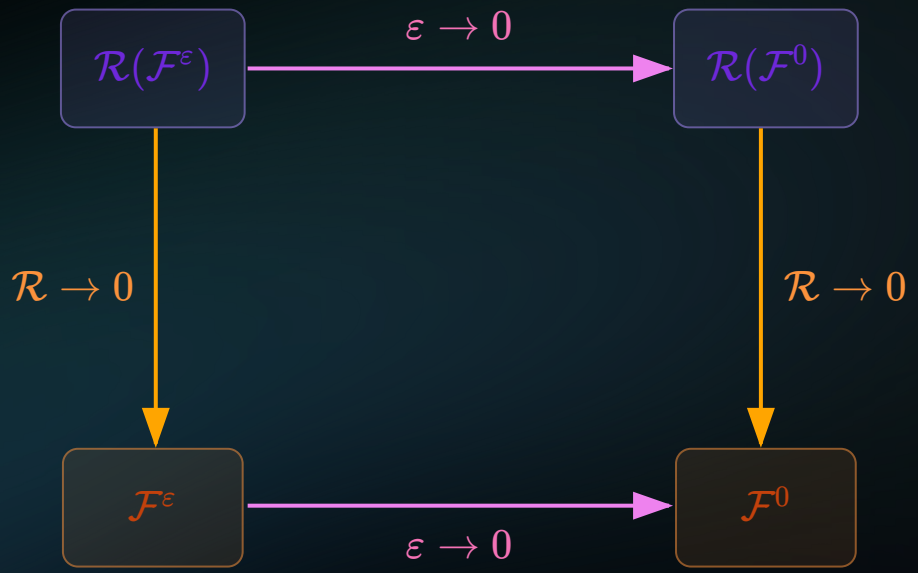

$\mathcal{F}^\varepsilon,\ \mathcal{F}^0$ Microscopic and macroscopic models

$\mathcal{R}(\mathcal{F}^\varepsilon),\ \mathcal{R}(\mathcal{F}^0)$ Loss of microscopic and macroscopic models

Micro-macro System

Classical numerical schemes based on this system are usually AP schemes

The micro-macro system for the linear trasport equation

$$\begin{cases} \partial_t \rho + \langle v \cdot \nabla_x g \rangle = 0, \\ \\ \varepsilon^2 \partial_t g + \varepsilon \left(I - \Pi \right) \left(v \cdot \nabla_x g \right) + v \cdot \nabla_x \rho = -g. \end{cases}$$

Sending $\varepsilon \to 0$, the above system formally approaches

$$\begin{cases} \partial_t \rho + \langle v \cdot \nabla_x g \rangle = 0, \\ -v \cdot \nabla_x \rho = g. \end{cases}$$

Plugging the second equation into the first equation gives the diffusion equation

$$\rho_t - \frac{1}{3} \rho_{xx} = 0.$$

APNN v1: based on Micro-macro decomposition

Re-design of loss

$$\mathcal{R}^{\varepsilon}_{\mathrm{APNN}} = \int \left(\partial_t \rho_\theta^{\mathrm{NN}} + \nabla_x \cdot \left\langle v g_\theta^{\mathrm{NN}} \right\rangle\right)^2 \mathrm{d}x\mathrm{d}t$$
$$+ \int \left|\varepsilon^2 \partial_t g_\theta^{\mathrm{NN}} + \varepsilon (I - \Pi)(v \cdot \nabla_x g_\theta^{\mathrm{NN}}) \quad + v \cdot \nabla_x \rho_\theta^{\mathrm{NN}} + g_\theta^{\mathrm{NN}}\right|^2 \mathrm{d}v\mathrm{d}x\mathrm{d}t$$

Let $\varepsilon \to 0$, the loss converges to

$$\mathcal{R}^{0}_{\mathrm{APNN}} = \int \left(\partial_t \rho_\theta^{\mathrm{NN}} + \nabla_x \cdot \left\langle v g_\theta^{\mathrm{NN}} \right\rangle\right)^2 \mathrm{d}x\mathrm{d}t + \int \left(v \cdot \nabla_x \rho_\theta^{\mathrm{NN}} + g_\theta^{\mathrm{NN}}\right)^2 \mathrm{d}v\mathrm{d}x\mathrm{d}t.$$

APNN v1: based on Micro-macro decomposition

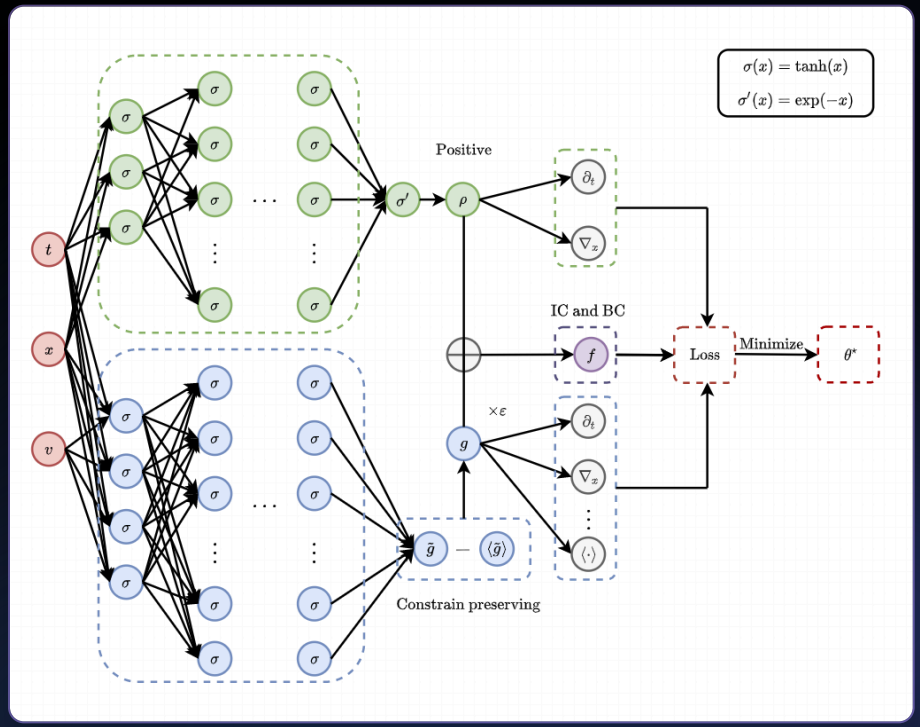

Mass conservation mechanism $g_\theta^{\mathrm{NN}} = \tilde{g}_\theta^{\mathrm{NN}} - \langle \tilde{g}_\theta^{\mathrm{NN}} \rangle$ is also important!

Test examples

Periodic boundary condition: $\varepsilon = 1$

$$f(t, x_L, v) = f(t, x_R, v),$$
$$f_0(x, v) = \frac{1 + \cos(4\pi x)}{\sqrt{2\pi}} e^{-\frac{v^2}{2}}.$$

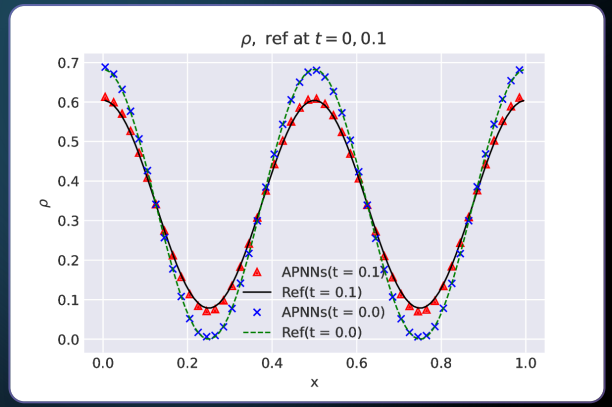

Inflow boundary condition $\varepsilon = 10^{-8}$

$$f(t, x_L, v) = 1 \text{ for } v > 0 \text{ and } 1 \text{ for } v < 0,$$
$$f_0(x, v) = 0.$$

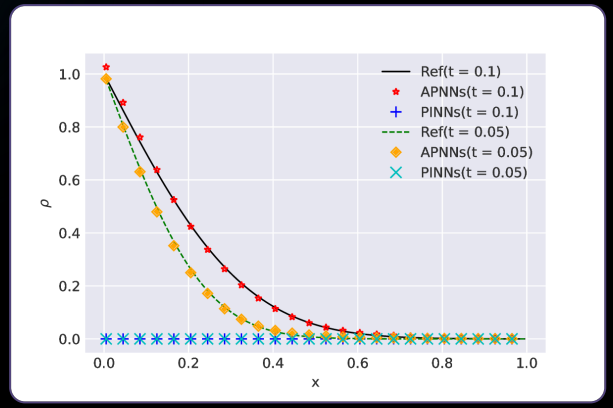

One can observed that APNN works for both $\varepsilon = 1$ and $\varepsilon = 10^{-8}$.

Mass conservation mechanism

Ex 3: Inflow boundary condition ($\varepsilon = 10^{-8}$)

For the constraint $\langle g \rangle = 0$, one way is to construct a novel neural network for g such that it exactly satisfies $\langle g \rangle = 0$.

The other way is to treat it as a soft constraint with parameter λ_3, we use $\hat{g}_\theta^{\mathrm{NN}}$ and modifies the loss as

$$\mathcal{R}_{\mathrm{APNN}} + \lambda_3 \int |\langle \hat{g}_\theta^{\mathrm{NN}} \rangle - 0|^2 \mathrm{d}x\mathrm{d}t.$$

Plot of density ρ at $t = 0.1$: APNNs with soft constraint (marker) vs. Ref (line).

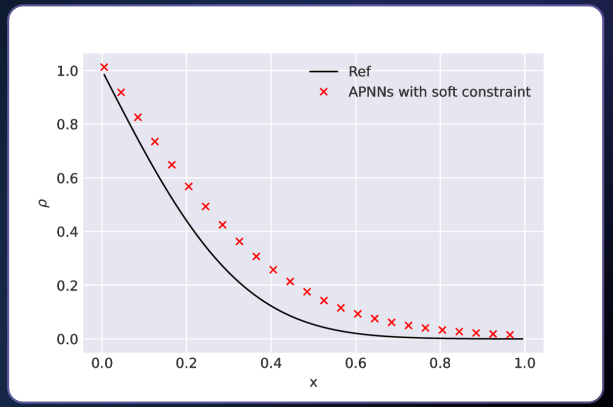

Mass conservation mechanism $g_\theta^{\mathrm{NN}} = \tilde{g}_\theta^{\mathrm{NN}} - \langle \tilde{g}_\theta^{\mathrm{NN}} \rangle$ is important!

Even and odd parity method

Alternative method for constructing AP schemes in classical numerical methods

$$\varepsilon\partial_t f + v\cdot\nabla_x f = \frac{1}{\varepsilon}\left(\frac{1}{2}\int_{-1}^{1} f\mathrm{d}v' - f\right),\ -1\le v\le 1$$

By splitting equation and define even- and odd-parities as

$$r(t,x,v) = \frac{1}{2}[f(t,x,v)+f(t,x,-v)],\ 0\le v\le 1,$$
$$j(t,x,v) = \frac{1}{2\varepsilon}[f(t,x,v)-f(t,x,-v)],\ 0\le v\le 1,$$

one can obtain

$$\begin{cases}\partial_t r + v\partial_x j = \dfrac{1}{\varepsilon^2}(\rho - r),\\ \partial_t j + \dfrac{1}{\varepsilon^2}v\partial_x r = -\dfrac{1}{\varepsilon^2}j,\end{cases}$$

where $\rho = \langle r\rangle := \int_0^1 r(t,x,v)\mathrm{d}v$.

Even and odd parity method

Not all traditional AP schemes work for neural networks!

$$\begin{cases} \partial_t r + v\partial_x j = \dfrac{1}{\varepsilon^2}(\rho - r), \\ \partial_t j + \dfrac{1}{\varepsilon^2} v\partial_x r = -\dfrac{1}{\varepsilon^2} j. \end{cases}$$

So far, we've got the even-odd system, however, it is not AP when applying neural networks for r and j.

To make it AP, we next introduce ρ into this system as a bridge between r and j.

By integrating over v, the first equation gives

$$\partial_t \langle r \rangle + \int_0^1 v\partial_x j \mathrm{d}v = \frac{1}{\varepsilon^2}(\rho - \langle r \rangle),$$

and due to $\rho = \langle r \rangle$, one can write as follows

$$\partial_t \rho + \langle v\partial_x j \rangle = 0.$$

Even and odd parity method

The even-odd parity system for the linear trasport equation

$$\begin{cases} \partial_t r + v\partial_x j = \dfrac{1}{\varepsilon^2}(\rho - r), \\ \partial_t j + \dfrac{1}{\varepsilon^2} v\partial_x r = -\dfrac{1}{\varepsilon^2} j, \\ \partial_t \rho + \langle v\partial_x j \rangle = 0. \end{cases}$$

Sending $\varepsilon \to 0$, the above system formally approaches

$$\begin{cases} \rho = r, \\ v\partial_x r = -j, \\ \partial_t \rho + \langle v\partial_x j \rangle = 0. \end{cases}$$

Plugging the first two equations into the third equation gives the diffusion equation $\rho_t - \frac{1}{3}\rho_{xx} = 0$.

APNN v2: based on even and odd parity

More general approach

The equation of local conservation law $\partial_t \rho + \langle v \partial_x j \rangle = 0$ is important in constructing the APNN loss. By coupling these equations of r, j and ρ, one can obtain the loss for the diffusion limit equation.

For solving the linear transport equation by deep neural networks, we need to use DNN to parametrize three functions $\rho(t,x), r(t,x,v)$ and $j(t,x,v)$.

So here three networks are used:

$$\rho_\theta^{\mathrm{NN}}(t,x) := \exp\left(-\tilde{\rho}_\theta^{\mathrm{NN}}(t,x)\right) \approx \rho(t,x),$$

$$r_\theta^{\mathrm{NN}}(t,x,v) := \exp\left(-\frac{1}{2}(\tilde{r}_\theta^{\mathrm{NN}}(t,x,v) + \tilde{r}_\theta^{\mathrm{NN}}(t,x,-v))\right) \approx r(t,x,v),$$

$$j_\theta^{\mathrm{NN}}(t,x,v) := \tilde{j}_\theta^{\mathrm{NN}}(t,x,v) - \tilde{j}_\theta^{\mathrm{NN}}(t,x,-v) \approx j(t,x,v).$$

APNN v2: based on even- and odd- parity

$$
\begin{aligned}
\mathcal{R}^{\varepsilon}_{\mathrm{APNN}} = \lambda_1 &\int |\varepsilon^2 \partial_t r_\theta^{\mathrm{NN}} + \varepsilon^2 v \partial_x j_\theta^{\mathrm{NN}} - (\rho_\theta^{\mathrm{NN}} - r_\theta^{\mathrm{NN}})|^2 \mathrm{d}v\mathrm{d}x\mathrm{d}t \\
+ \lambda_2 &\int |\varepsilon^2 \partial_t j_\theta^{\mathrm{NN}} + v \partial_x r_\theta^{\mathrm{NN}} - (-j_\theta^{\mathrm{NN}})|^2 \mathrm{d}v\mathrm{d}x\mathrm{d}t \\
+ \lambda_3 &\int |\partial_t \rho_\theta^{\mathrm{NN}} + \left\langle v \partial_x j_\theta^{\mathrm{NN}} \right\rangle|^2 \mathrm{d}x\mathrm{d}t \\
+ \lambda_4 &\int |\rho_\theta^{\mathrm{NN}} - \left\langle r_\theta^{\mathrm{NN}} \right\rangle|^2 \mathrm{d}x\mathrm{d}t
\end{aligned}
$$

Notice that the constraint $\rho = \langle r \rangle$ is also added into the APNN loss.

Test examples - Case I

Inflow boundary condition ($\varepsilon = 10^{-3}$)

$$
\begin{aligned}
f(t, x_L, v) &= 1 \text{ for } v > 0, \\
f(t, x_R, v) &= 0 \text{ for } v < 0, \\
\rho_0(x) &= 0, \\
f_0(x, v) &= 0.
\end{aligned}
$$

Note that the function f has a jump at $t = 0$ since $F_L(v) = 1, F_R(v) = 0$ but $f_0(x, v) = 0$.

For better numerical performance, $\rho_\theta^{\mathrm{NN}}$ can be further constructed to automatically satisfies initial condition:

$$\rho_\theta^{\mathrm{NN}}(t, x) := t \cdot \exp\left(-\tilde{\rho}_\theta^{\mathrm{NN}}(t, x)\right) \approx \rho(t, x)$$

Plot of density ρ at $t = 0, 0.05, 0.1$: APNNs (marker) vs. Ref (line).

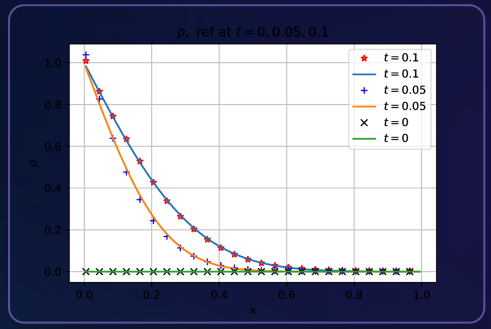

Relative ℓ^2 error of APNNs is 9.87×10^{-3}.

The numerical performance of enforcement of initial condition and the soft constraint $\rho = \langle r \rangle$ are discussed as follows.

Plot of density ρ at $t = 0, 0.05, 0.1$: APNNs (marker) vs. Ref (line).

Figure 1: without the enforcement of initial condition

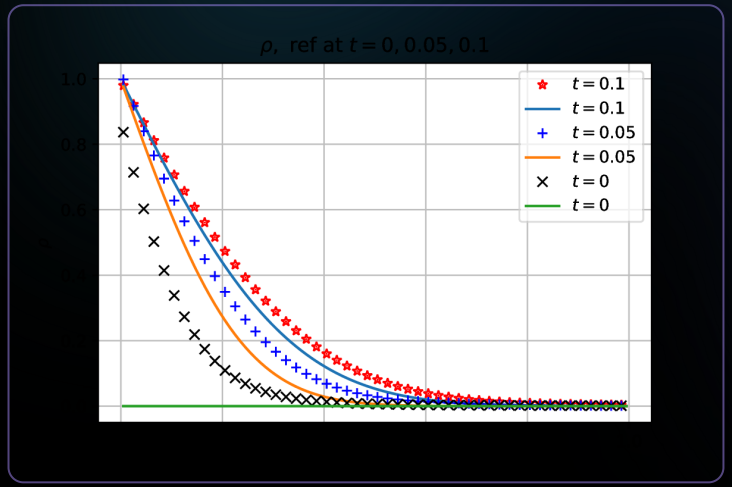

Due to the poor approximate of initial and boundary layer effect, it gives wrong solution at time $t = 0, 0.05, 0.1$.

Figure 2: without the constraint $\rho = \langle r \rangle$

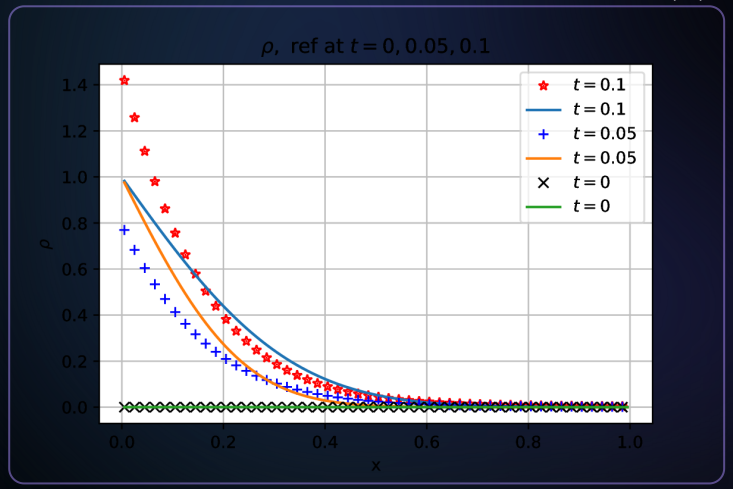

The solutions are also wrong at time $t = 0, 0.05, 0.1$, therefore, we consider this constraint into our APNN loss.

Test examples - Case II

UQ problems with inflow condition ($\varepsilon = 10^{-5}$)

$$\varepsilon \partial_t f + v \partial_x f = \frac{\sigma_S(\boldsymbol{z})}{\varepsilon} \left(\frac{1}{2} \int_{-1}^{1} f \, dv' - f \right), \quad x_L < x < x_R, \quad -1 \le v \le 1,$$

$$\sigma_S(\boldsymbol{z}) = 1 + \frac{1}{10} \prod_{i=1}^{20} \sin(\pi z^i), \ \boldsymbol{z} = (z^1, z^2, \cdots, z^{20}) \sim \mathcal{U}([-1,1]^{20}),$$

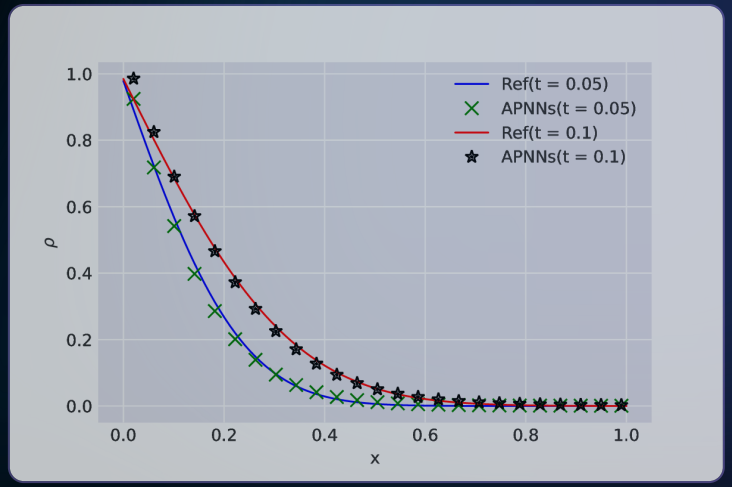

Bhatnagar-Gross-Krook (BGK) equation

$$\partial_t f + v \cdot \nabla_x f = \frac{1}{\varepsilon}\left(M(U) - f\right), \quad v \in \mathbb{R},$$

where $M(U)$ denotes the local Maxwellian distribution function given by

$$M(U) = \frac{\rho}{(2\pi T)^{\frac{1}{2}}} \exp\left(-\frac{|v-u|^2}{2T}\right),$$

and $\rho(t,x), u(t,x)$ and $T(t,x)$ are the density, macroscopic velocity and temperature which are related with the moments of f:

$$U := \begin{pmatrix} \rho \\ \rho u \\ \frac{1}{2}\rho|u|^2 + \frac{1}{2}\rho T \end{pmatrix} = \int_{\mathbb{R}} m f \mathrm{d}v, \; m = \left(1, v, \frac{1}{2}v^2\right)^T.$$

Notice that the Boltzmann-BGK equation is an integro-differential equation with its nonlinear and non-local collision operator.

Density, macroscopic velocity and temperature

- density

$$\rho = \int f(t,x,v)\mathrm{d}v.$$

- velocity

$$u = \int v \cdot \frac{f(t,x,v)}{\int f(t,x,v)\mathrm{d}v}\mathrm{d}v = \frac{1}{\rho}\int v f \mathrm{d}v.$$

- thermodynamics energy

$$\int \frac{1}{2}(v-u)^2 \cdot \frac{f(t,x,v)}{\int f(t,x,v)\mathrm{d}v}\mathrm{d}v = \frac{1}{\rho}\left[\frac{1}{2}\int v^2 f \mathrm{d}v - \frac{1}{2}\rho u^2\right],$$

$$\Rightarrow \frac{1}{2}\rho T = \frac{1}{2}\int_{\mathbb{R}} v^2 f \mathrm{d}v - \frac{1}{2}\rho|u|^2 \ (\text{The ideal gas law}).$$

Local conservation laws

$$\partial_t f + v \cdot \nabla_x f = \frac{1}{\varepsilon}\left(M(U) - f\right), \quad v \in \mathbb{R},$$

$$U := \begin{pmatrix} \rho \\ \rho u \\ \frac{1}{2}\rho|u|^2 + \frac{1}{2}\rho T \end{pmatrix} = \int_{\mathbb{R}} m f \mathrm{d}v, \; m = \left(1, v, \frac{1}{2}v^2\right)^T.$$

Due to the properties of conserving mass, momentum and energy of collision operator, one can multiply the BGK equation by $m(v)$ and integrate with respect to v to obtain the equations of local conservation laws

$$\partial_t \langle m f \rangle + \nabla_x \cdot \langle v m f \rangle = 0, \text{ where } \langle g \rangle = \int_{\mathbb{R}} g(v) \mathrm{d}v,$$

i.e.,

$$\partial_t \begin{pmatrix} \rho \\ \rho u \\ \frac{1}{2}\rho|u|^2 + \frac{1}{2}\rho T \end{pmatrix} + \nabla_x \cdot \langle v m f \rangle = 0.$$

APNN System

The systems of Boltzmann-BGK model

$$\begin{cases} \varepsilon\left(\partial_t f + v\partial_x f\right) = M(U) - f, \\ \partial_t \begin{pmatrix} \rho \\ \rho u \\ \frac{1}{2}\rho|u|^2 + \frac{1}{2}\rho T \end{pmatrix} + \nabla_x \cdot \langle vmf \rangle = 0, \\ \begin{pmatrix} \rho \\ \rho u \\ \frac{1}{2}\rho|u|^2 + \frac{1}{2}\rho T \end{pmatrix} = \int_{\mathbb{R}} mf \mathrm{d}v. \end{cases}$$

Sending $\varepsilon \to 0$, one have $f = M(U)$ and the local conservation laws becomes compressible Euler equation:

$$\partial_t \begin{pmatrix} \rho \\ \rho u \\ \frac{1}{2}\rho|u|^2 + \frac{1}{2}\rho T \end{pmatrix} + \nabla_x \cdot \langle vmM \rangle = 0.$$

Boundary and initial conditions

The boundary conditions of ρ, u, T are set as constants:

$$\begin{aligned}
&\rho(t, x_L) = \rho_L, \rho(t, x_R) = \rho_R, \\
&u(t, x_L) = u_L = 0, u(t, x_R) = u_R = 0, \\
&T(t, x_L) = T_L, T(t, x_R) = T_R.
\end{aligned}$$

The initial condition of f is computed by the initial functions $\rho_0(x), u_0(x), T_0(x)$:

$$f(0, x, v) = \frac{\rho_0}{(2\pi T_0)^{\frac{1}{2}}} \exp\left(-\frac{|v - u_0|^2}{2T_0}\right) := f_0(x, v).$$

Here, time $t \in \mathcal{T} := [0, T]$, space point $x \in \mathcal{D} := [x_L, x_R]$ and we restrict the range of velocity to a bounded symmetrical domain $\Omega = [-V, V]$ with $V = 10$ since this assumption might be realistic in many studies.

APNN v2 for Boltzmann-BGK equation

First we parametrize four functions $f(t,x,v), \rho(t,x), u(t,x)$ and $T(t,x)$ with four networks. The time and velocity variable t, v are normalized into $[0,1]$ and $[-1,1]$ with scaling $\bar{t} = t/T, \bar{v} = v/V$ and we construct four DNNs as follows:

$$f_\theta^{\mathrm{NN}}(t,x,v) := \ln\left(1+\exp(\tilde{f}_\theta^{\mathrm{NN}}(\bar{t},x,\bar{v}))\right) > 0,$$

$$\rho_\theta^{\mathrm{NN}}(t,x) := \exp\left((x-x_L)(x_R-x)\cdot\tilde{\rho}_\theta^{\mathrm{NN}}(\bar{t},x) + \log(\rho_L)\frac{x_R-x}{x_R-x_L} + \log(\rho_R)\frac{x-x_L}{x_R-x_L}\right) > 0,$$

$$u_\theta^{\mathrm{NN}}(t,x) := \sqrt{(x-x_L)(x_R-x)}\cdot\tilde{u}_\theta^{\mathrm{NN}}(\bar{t},x),$$

$$T_\theta^{\mathrm{NN}}(t,x) := \exp\left((x-x_L)(x_R-x)\cdot\tilde{T}_\theta^{\mathrm{NN}}(\bar{t},x) + \log(T_L)\frac{x_R-x}{x_R-x_L} + \log(T_R)\frac{x-x_L}{x_R-x_L}\right) > 0,$$

which $\rho_\theta^{\mathrm{NN}}, u_\theta^{\mathrm{NN}}, T_\theta^{\mathrm{NN}}$ automatically satisfy the boundary conditions. In this problem, to keep f positive, $\ln(1+\exp(\cdot))$ is applied for constructing f_θ^{NN}. The benefit of this construction is that the values of f_θ^{NN} and $\tilde{f}_\theta^{\mathrm{NN}}$ are at the same level.

APNN loss for Boltzmann-BGK

$$
\begin{aligned}
\mathcal{R}^{\varepsilon}_{\text{APNN, BGK}} = & \frac{\lambda_1}{N_1^{(1)}} \sum_{i=1}^{N_1^{(1)}} \left| \varepsilon(\partial_t f_\theta^{\text{NN}}(t_i, x_i, v_i) + v \nabla_x f_\theta^{\text{NN}}(t_i, x_i, v_i)) - \left(M(U_\theta^{\text{NN}}) - f_\theta^{\text{NN}}\right)(t_i, x_i, v_i) \right|^2 \\
& + \frac{\lambda_2}{N_1^{(2)}} \sum_{i=1}^{N_1^{(2)}} \left| \partial_t \rho_\theta^{\text{NN}}(t_i, x_i) + \nabla_x \left\langle v f_\theta^{\text{NN}} \right\rangle (t_i, x_i) \right|^2 \\
& + \frac{\lambda_3}{N_1^{(3)}} \sum_{i=1}^{N_1^{(3)}} \left| \partial_t (\rho_\theta^{\text{NN}}(t_i, x_i) u_\theta^{\text{NN}}(t_i, x_i)) + \nabla_x \left\langle v^2 f_\theta^{\text{NN}} \right\rangle (t_i, x_i) \right|^2 \\
& + \frac{\lambda_4}{N_1^{(4)}} \sum_{i=1}^{N_1^{(4)}} \left| \partial_t \left(\frac{1}{2} \rho_\theta^{\text{NN}}(t_i, x_i) (u_\theta^{\text{NN}}(t_i, x_i))^2 + \frac{1}{2} \rho_\theta^{\text{NN}}(t_i, x_i) T_\theta^{\text{NN}}(t_i, x_i) \right) + \right. \\
& \qquad \left. \nabla_x \left\langle \frac{1}{2} v^3 f_\theta^{\text{NN}} \right\rangle (t_i, x_i) \right|^2
\end{aligned}
$$

Test example

Initial conditions ($\varepsilon = 10^{-3}$)

$$\rho_0(x) = 1.5 + (0.625 - 1.5) \cdot \frac{\sin(\pi x) + 1}{2},$$
$$u_0(x) = 0,$$
$$T_0(x) = 1.5 + (0.75 - 1.5) \cdot \frac{\sin(\pi x) + 1}{2},$$

$$f_0(x, v) = \frac{\rho_0}{(2\pi T_0)^{\frac{1}{2}}} \exp\left(-\frac{|v - u_0|^2}{2T_0}\right).$$

The reference solutions are the density, momentum and energy:

$$\rho, \rho u, \frac{1}{2}\rho u^2 + \frac{1}{2}\rho T.$$

Setting: ResNet with units $[3, 128, 128, 128, 128, 128, 128, 1]$ for f and $[2, 64, 64, 64, 64, 64, 64, 1]$ both for ρ, u and T. Batch size is 512 in domain, and 256 on initial, the number of quadrature points is 64.

$\lambda_9 = 0.1, \lambda_{11} = \lambda_{13} = \lambda_{14} = 10$ and others are set to be 1.

For $t = 0$: mean square error of density, momentum and energy are $7.16\text{e-}8, 4.50\text{e-}6, 8.13\text{e-}7$.

For $t = 0.1$: relative l^2 error of density, momentum and energy are $5.43\text{e-}3, 6.35\text{e-}3, 4.47\text{e-}2$.

The integrals of approximate f and approximate density, momentum and energy at time $t = 0$

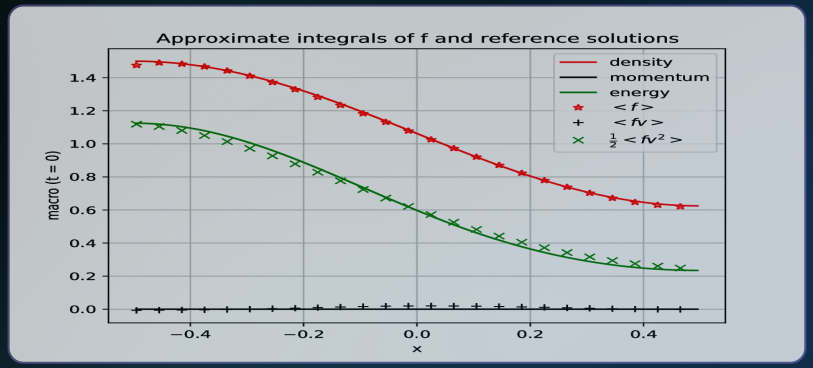

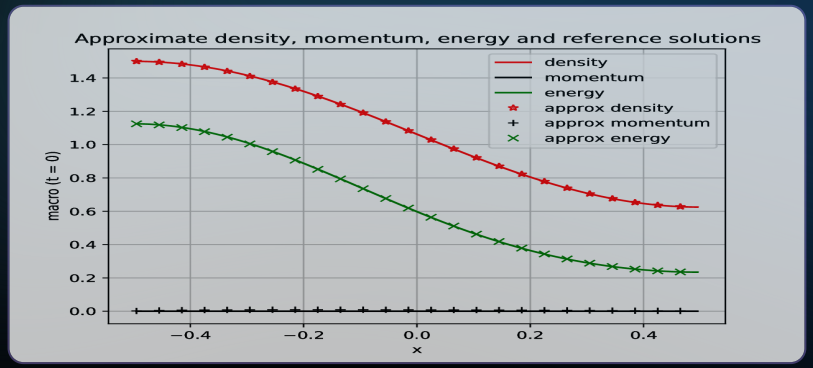

The integrals of approximate f and approximate density, momentum and energy at time $t = 0.1$

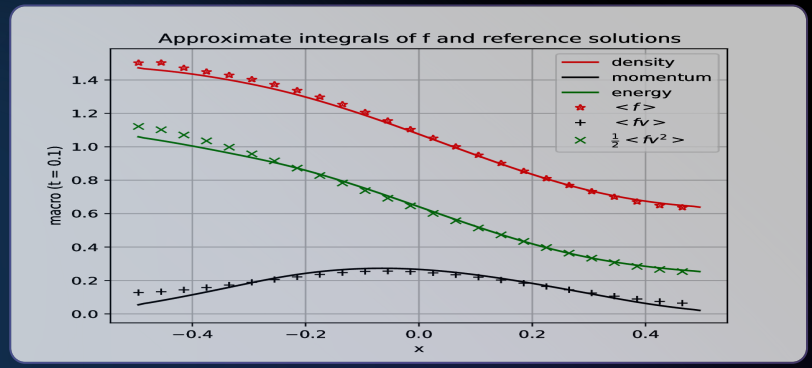

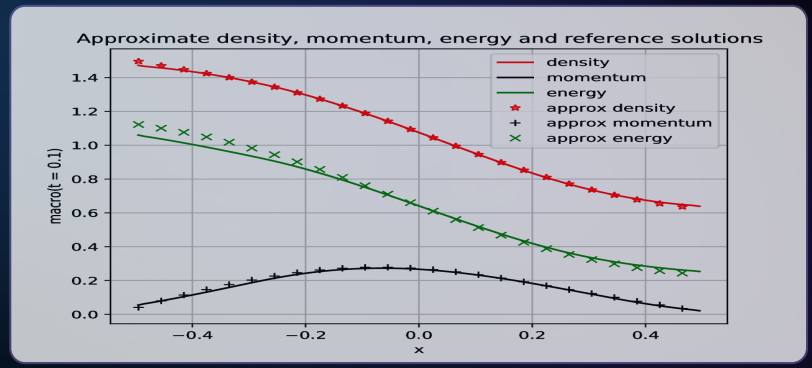

APNN for More General Systems

VPFP, Gray-RTE, etc.

APNNs for Vlasov-Poisson-Fokker-Planck system

VPFP System

$$\partial_t f + v \cdot \nabla_x f - \frac{1}{\varepsilon} \nabla_x \phi \cdot \nabla_v f = \frac{1}{\varepsilon} \nabla_v \cdot [v f + \nabla_v f],$$
$$-\nabla_x \phi(t,x) = \rho(t,x) - h(x),$$

where

$$\rho(t,x) = \int_{\mathbb{R}^N} f(t,x,v) \mathrm{d}v$$

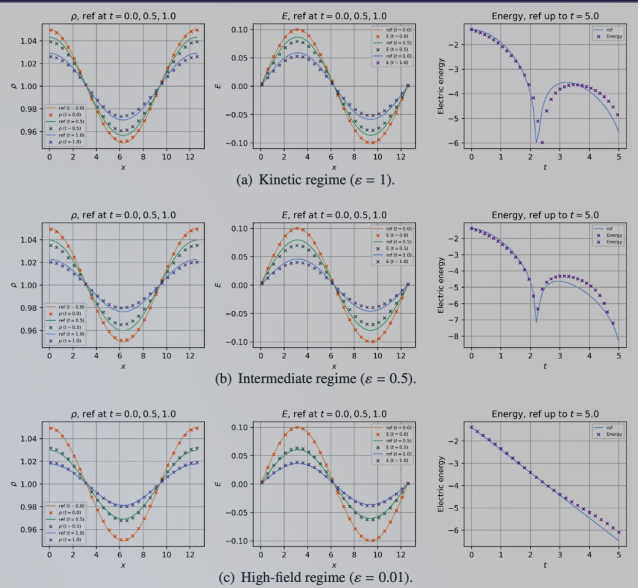

(a) Kinetic regime ($\varepsilon = 1$).

(b) Intermediate regime ($\varepsilon = 0.5$).

(c) High-field regime ($\varepsilon = 0.01$).

Figure 2: Multiscale linear Landau damping solved by the mass conservation based APNN method. Density ρ (left column) and electric field E (middle column) as functions of space x at $t = 0.0, 0.5, 1.0$; electric energy (right column) as a function of time t up to $t = 5.0$. Neural networks are $[3, 128, 128, 128, 128, 128, 1]$ for ρ, ϕ and $[4, 256, 256, 256, 256, 256, 1]$ for f. Batch size is 512 in domain and 256 for initial condition and 256 for conservation condition $\rho = \langle f \rangle$. Penalty $\kappa_1 = 120$, $\kappa_3 = \kappa_4 = 1$ for kinetic regime; penalty $\kappa_1 = 150$, $\kappa_3 = \kappa_4 = 1$ for intermediate regime; and penalty $\kappa_1 = 500$, $\kappa_3 = \kappa_4 = 1$ for high-field regime.

APNNs for GRTE

APNNs for Multiscale Gray Radiative Transfer Equations

Original system

$$
\begin{cases}
\dfrac{\varepsilon^2}{c}\dfrac{\partial I}{\partial t} + \varepsilon\Omega\cdot\nabla I = \sigma\left(\dfrac{1}{4\pi}acT^4 - I\right), \\
\varepsilon^2 C_v \dfrac{\partial T}{\partial t} = \sigma\left(\displaystyle\int_{S^2} I\mathrm{d}\Omega - acT^4\right), \\
\mathcal{B}I = 0, \\
I(t=0,x,\Omega) = I_0(x,\Omega), \\
T(t=0,x) = T_0(x),
\end{cases}
$$

APNN based on even-odd decomposition

$$
\begin{cases}
\dfrac{\varepsilon^2}{c}\partial_t r + \dfrac{\varepsilon^2}{\sqrt{\sigma_0}}\cdot\mu\partial_x j = \sigma\left(\dfrac{1}{2}acT^4 - r\right), \\
\dfrac{\varepsilon^2}{c\sqrt{\sigma_0}}\partial_t j + \mu\partial_x r = -\dfrac{\sigma}{\sqrt{\sigma_0}} j, \\
\dfrac{1}{c}\partial_t \rho + \dfrac{1}{\sqrt{\sigma_0}}\cdot\langle\mu\partial_x j\rangle = -\dfrac{1}{2}C_v\dfrac{\partial T}{\partial t}, \\
\varepsilon^2 C_v \dfrac{\partial T}{\partial t} = \sigma\left(2\rho - acT^4\right), \\
\rho = \langle r\rangle .
\end{cases}
$$

APNNs for GRTE

Numerics and schema

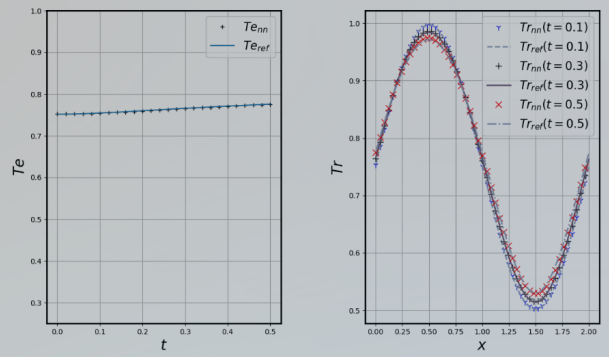

Figure 5: Plot of the approximated material temperature $T_e = T$ at space $x = 0.0025$ and the radiation temperature T_r at time $t = 0.1, 0.3, 0.5$ with APNN based on micro-macro decomposition under the kinetic regime.

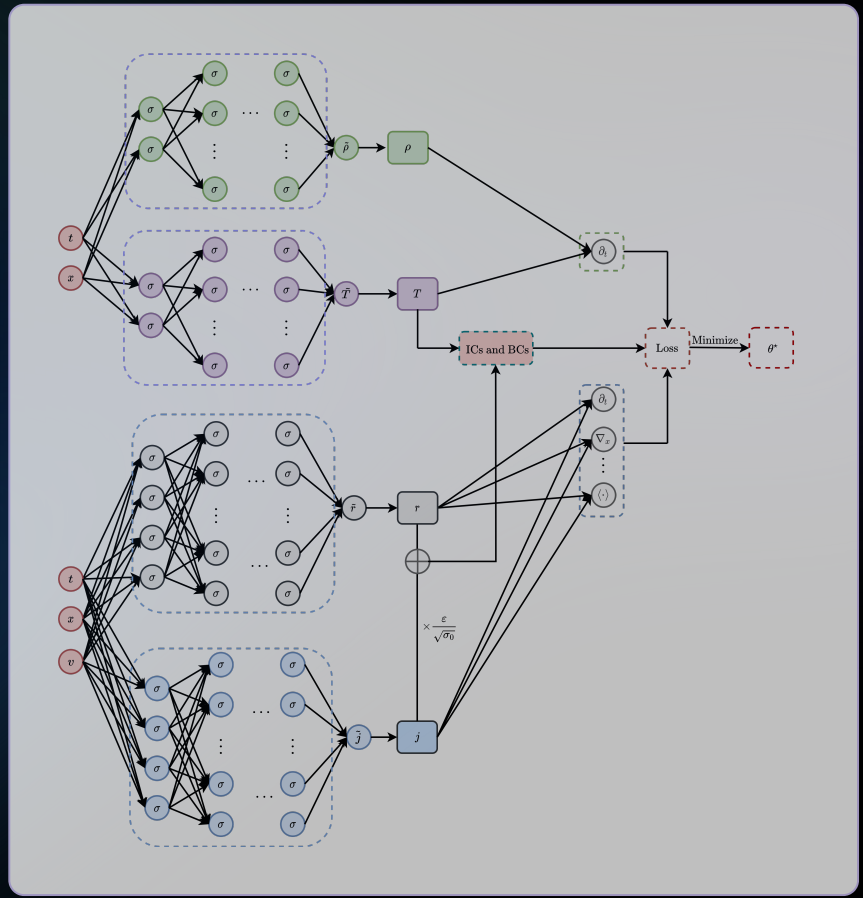

RT-APNNs: ResNet

With 3 key improvements to APNNs

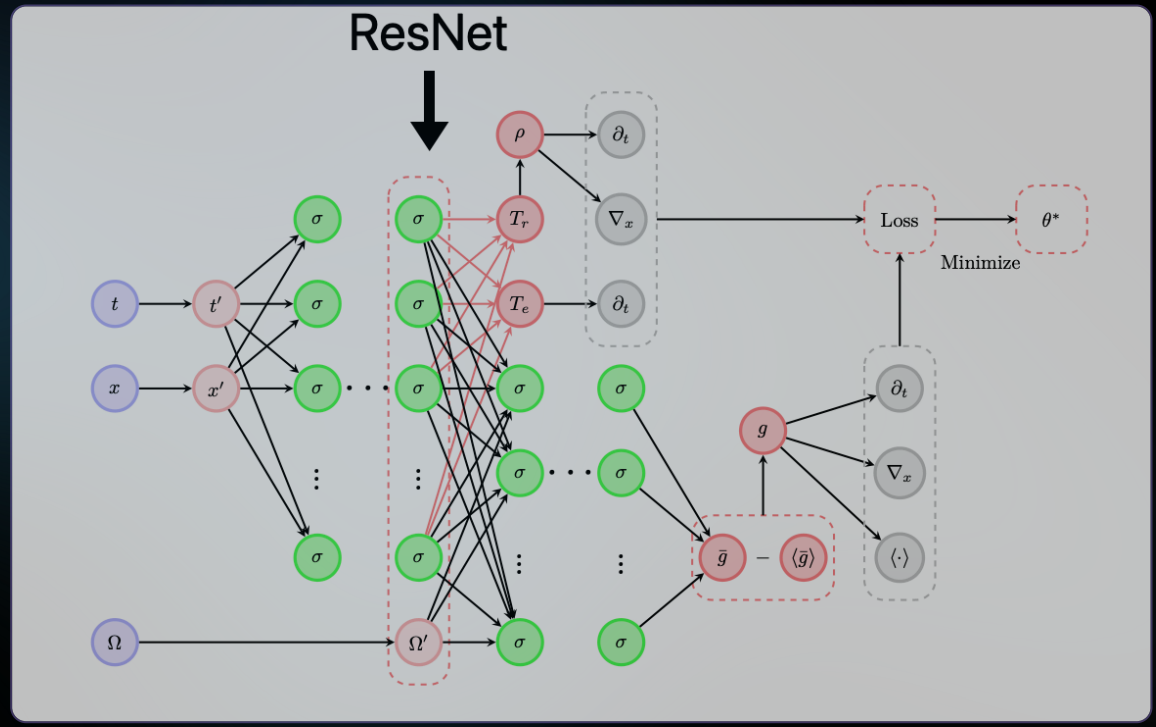

RT-APNNs: Pre-training

With 3 key improvements to APNNs

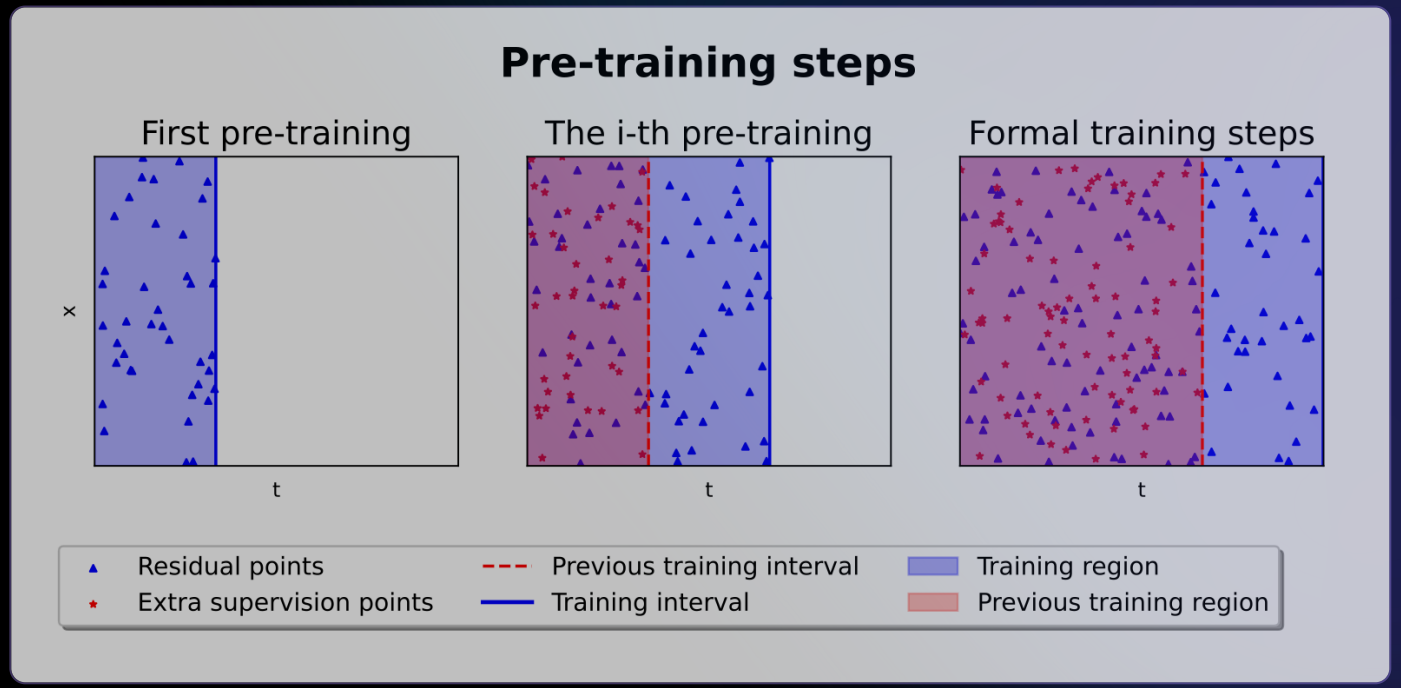

Improve the long time stability

RT-APNNs: MCMC

With 3 key improvements to APNNs

Algorithm 1 Adaptive sampling in MCMC [54].

Require: Initial points $\{(t_j^{(0)}, x_j^{(0)})\}_{j=1}^{N_r}$, upper bound U_b, lower bound L_b, Update function U,Indicator function π, step size ϵ, steps N_{mcmc}.

for $j = 1$ to N_r **do**
  for $i = 1$ to N_{mcmc} **do**
    Generate u from $\mathcal{U}[0, 1]$.
    Sample new intermediate state $(t', x') \sim \mathcal{N}((t_j^{(i-1)}, x_j^{(i-1)}), \Sigma)$,
    Map to new proposal state: $(t^*, x^*) = U(t', x')$.
    Calculate acceptance probability:

$$\alpha\left(t_j^{(i-1)}, x_j^{(i-1)}; t^*, x^*\right) = \min\left\{1, \frac{\pi\left(t_j^{(i-1)}, x_j^{(i-1)}\right)}{\pi\left(t^*, x^*\right)}\right\} \tag{3.3.3}$$

    if $u < \alpha(\boldsymbol{t}_j^{(i-1)}, x_j^{(i-1)}; \boldsymbol{t}^*, x^*)$ **then**
      Accept proposal: $(\boldsymbol{t}_j^{(i)}, x_j^{(i)}) = (\boldsymbol{t}^*, x^*)$.
    else
      Reject proposal: $(\boldsymbol{t}_j^{(i)}, x_j^{(i)}) = (\boldsymbol{t}_j^{(i-1)}, x_j^{(i-1)})$.
    end if
  end for
  Set $(t_j, x_j) = (t_j^{(N_{\text{mcmc}})}, x_j^{(N_{\text{mcmc}})})$.
end for

Ensure: The newly obtained collocation points

Improve the Sampling efficiency

RT-APNNs Result: Marshak Wave

ResNet + Pre-training + MCMC

Table 2: The relative L^2 error of ρ at time $t = 0.04, 0.1, 0.3, 2.0$ for the diffusion regime ($\varepsilon = 10^{-8}$) in Ex 1 [26].

L^2 error	$t = 0.04$	$t = 0.1$	$t = 0.3$	$t = 2.0$
PINNs	$7.05e-01$	$7.57e-01$	$7.49e-01$	$3.63e-01$
APNNs	$4.54e-02$	$1.62e-02$	$5.31e-03$	$5.78e-03$
RT-APNN	$1.61e-02$	$4.73e-03$	$3.64e-03$	$1.55e-03$

Table 3: The relative L^2 error of ρ at times $t = 0.04, 0.1, 0.3, 2.0$ with Adam training 10,000 steps in the diffusion regime ($\varepsilon = 10^{-8}$) in Ex 1.

L^2 error	$t = 0.04$	$t = 0.1$	$t = 0.3$	$t = 2.0$
APNNs	$2.99e-02$	$9.14e-03$	$3.84e-03$	$4.54e-04$
APNNs+①	$1.24e-02$	$6.17e-03$	$4.02e-03$	$2.98e-03$
APNNs+①②	$1.34e-02$	$6.04e-03$	$6.10e-03$	$1.94e-03$
APNNs+①②③ (RT-APNN)	$1.55e-02$	$6.89e-03$	$2.33e-03$	$9.89e-04$

Obtain higher accuracy and efficiency, especially for long time simulation

APNN with Different Architectures

APRFMs, APCONs, etc.

APCONs: Operator Learning

APNN + Modified DeepONets

$$\begin{cases} \varepsilon \partial_t f + v \cdot \nabla_x f = \dfrac{1}{\varepsilon} \mathcal{L} f, \ (t, x, v) \in \mathcal{T} \times \mathcal{D} \times \Omega, \\ \mathcal{B} f(t, x, v) = 0, \\ f(0, x, v) = f_0(x, v). \end{cases}$$

Our goal is to learn the mapping $\mathcal{G}$ from

$$\mathcal{G} : f_0(x, v) \to f(t, x, v)$$

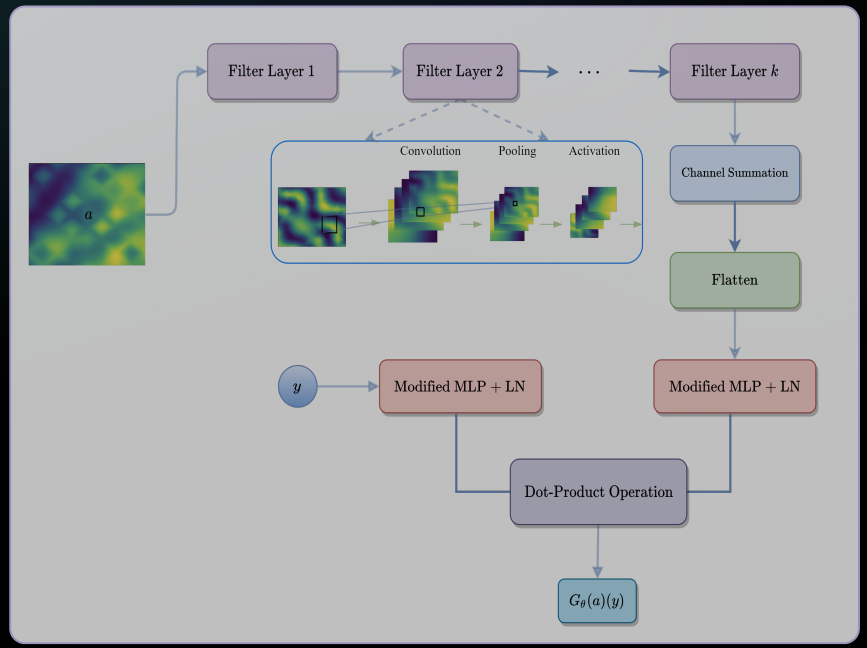

Convolutional DeepONets

Schematic of APCONs

APCON based on Micro-macro decomposition

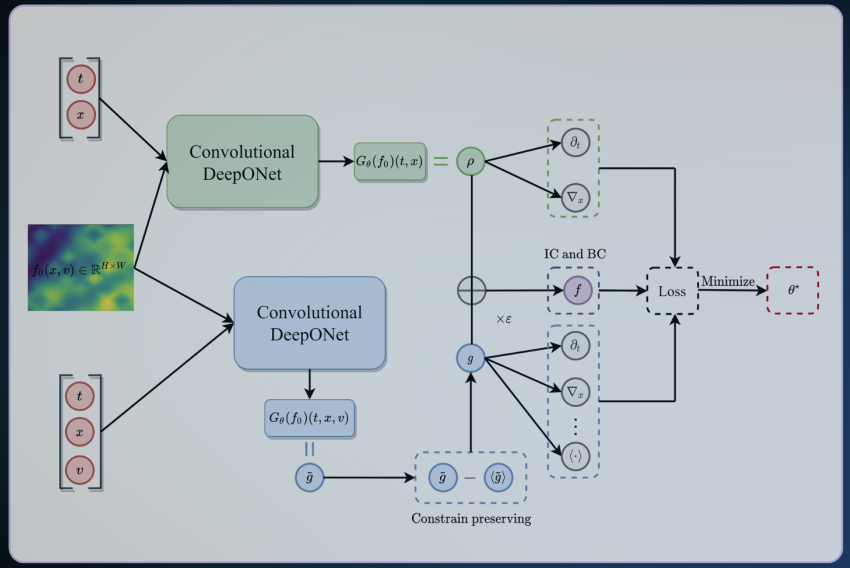

APCON based on even-odd decomposition

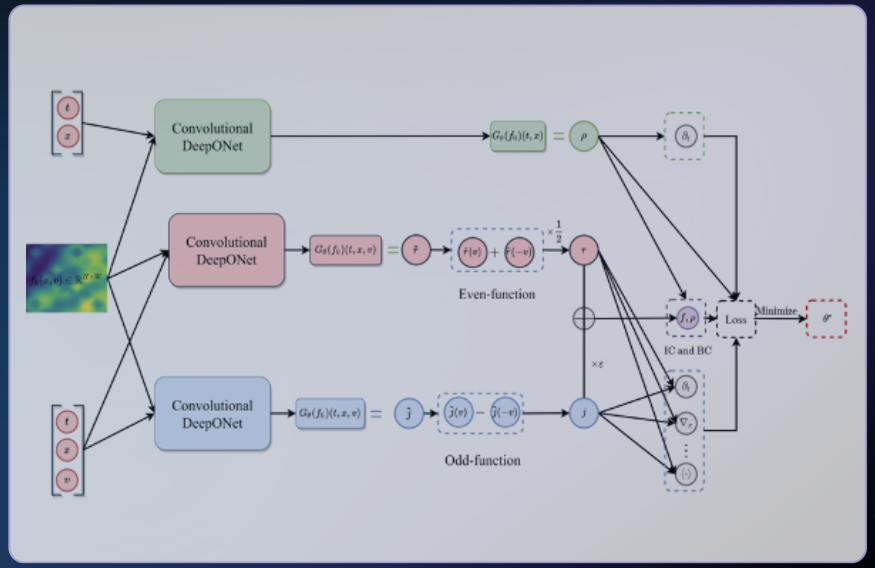

APCONs Performance

Accuracy and parameters

Table 1: Comparison in kinetic regime ($\varepsilon = 1$) of Problem I.

QoIs \ Method	PI		AP v1		AP v2	
	DON	CON	DON	CON	DON	CON
Relative ℓ^2 error	1.88 e-2	1.74 e-2	3.32 e-2	1.59 e-2	1.48 e-2	1.44 e-2
# params	423 296	43 288	846 400	86 384	1 269 696	129 672

Table 2: Comparison in the diffusion regime ($\varepsilon = 10^{-4}$) of Problem I.

QoI \ Method	PI		AP v1		AP v2	
	DON	CON	DON	CON	DON	CON
Relative ℓ^2 error	–	–	2.63e-2	1.58e-2	4.09e-2	1.55 e-2

APCON efficiency

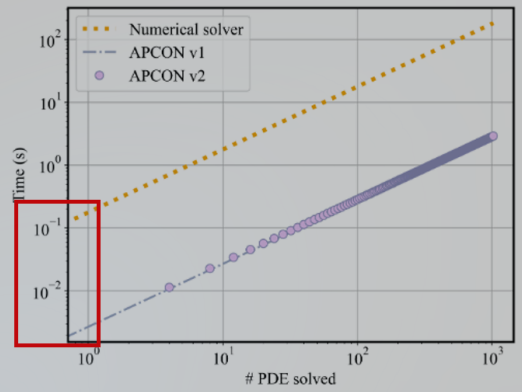

Figure 10: Computational cost (second) for performing inference with pre-trained APCONs, along with the corresponding time required to solve a PDE with a conventional fast spectral method which encompasses a scalable GPU implementation utilizing cupy. Reported timings are obtained on a single NVIDIA RTX 3090 graphics processing unit (GPU). The average total time costs for the classical numerical solver, APCON-v1, and APCON-v2 are 176.9 ms, 2.69 ms, and 2.85 ms, respectively.

With less paramers than PIDON, 100x faster than conventional numerical methods

Conclusions

- We proposed APNNs framwork for solving multiscale kinetic equations by deep learning:
  - Based on micro-macro decomposition: APNN v1
  - Based on odd-even parity method: APNN v1
  - Based on local conservation laws: APNN v2
  - Combined with ResNet, pre-training and MCMC: RT-APNNs
  - Combined with random feature methods: APRFMs
  - Combined with operator learning : APCONs
- APNNs can be applied to various multiscale kinetic equations, such as:
  - Linear transport equations
  - Boltzmann-BGK equation
  - Vlasov-Poisson-Fokker-Planck system
  - Gray radiative transfer equations
  - and more: full Boltzmann equations

References

- Keke Wu, Xizhe Xie, Wengu Chen, Han Wang and Zheng Ma, RT-APNN for Solving Gray Radiative Transfer Equations, *preprint*, 2025
- Jingru Chen, Zheng Ma and Keke Wu, A micro-macro decomposition-based asymptotic-preserving random feature method for multiscale radiative transfer equations, *Jounral of Computational Physics*, 2025
- Shi Jin, Zheng Ma and Keke Wu, Asymptotic-Preserving Neural Networks for Multiscale Kinetic Equations, *Communication in Computational Physics*, 2024
- Shi Jin, Zheng Ma and Tian-ai Zhang, Asymptotic-preserving neural networks for multiscale Vlasov-Poisson-Fokker-Planck system in the high-field, *Jounral of Scientific Computing*, 2024
- Keke Wu, Xiong-bin Yan, Shi Jin and Zheng Ma, Capturing the Diffusive Behavior of the Multiscale Linear Transport Equations by Asymptotic-Preserving Convolutional DeepONets, *Computer Methods in Applied Mechanics and Engineering* , 2024
- Shi Jin, Zheng Ma and Keke Wu, Asymptotic-Preserving Neural Networks for Multiscale Time-Dependent Linear Transport Equations, *Journal of Scientific Computing*, 2023

Thank You!

Slides can be found here